

## Wave-Induced Transport in the Pure Electron Plasma

J. S. deGrassie and J. H. Malmberg

*Department of Physics, University of California at San Diego, La Jolla, California 92093*

(Received 28 June 1977)

The pure electron plasma is an excellent system in which to study transport across a strong magnetic field. We describe the basic experimental arrangement and report on measurements of transport due to an externally launched diocotron mode.

Plasmas which consist of a single charge species<sup>1,2</sup> are of interest in their own right and for the investigation of basic interactions common to all plasmas. We have found<sup>3-5</sup> that the pure electron plasma is an excellent system in which to investigate transport across a strong magnetic field. Here we describe the basic experimental arrangement and report on observations of electron spatial transport due to an externally launched diocotron<sup>6,7</sup> mode.

We have previously described<sup>8</sup> a simple apparatus which produces a steady-state electron-plasma column which is many Debye lengths in diameter, and proved experimentally that the residual ion density is very small compared to the electron density; i.e., the plasma is almost purely

electrons. We now describe how the plasma may be trapped and used for investigation of transport. A schematic diagram of the apparatus is given in Fig. 1. The geometry is cylindrical. The entire system is immersed in a strong uniform axial magnetic field  $\vec{B}_0$  and evacuated to a base pressure of  $\sim 10^{-7}$  Torr. The system is pulsed repetitively in the following sequence: (1) Initially, conducting cylinder *A* is grounded and *C* is biased sufficiently negative to reflect all electrons coming from the negatively biased source. During this filling time ( $\tau_f$ ) the plasma occupies cylinders *A* and *B*. (2) Then the potential of cylinder *A* is gated negative<sup>9</sup> to cut off the incoming electrons and trap those within cylinder *B*. The trapped-electron plasma is radially confined by

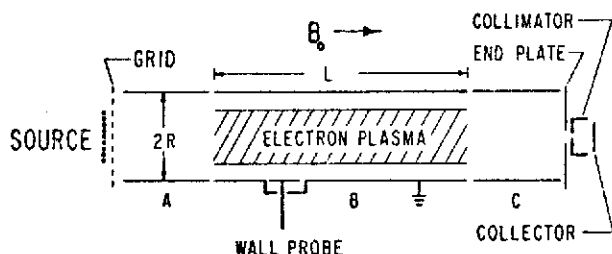


FIG. 1. Schematic of the apparatus. Five wall probes are located throughout cylinder B, they are 1.85 cm in axial length and 2.57 cm in arc. Other dimensions are the following:  $R = 3.40$  cm;  $L = 45.7$  cm; the collimator diameter is 3.05 mm.

the magnetic field and axially confined by the electrostatic fields of the end cylinders, which are sufficiently negative that it is energetically impossible for the electrons to escape from the ends. The electrons then wander across the magnetic-field lines because of various processes. Some reach the wall of cylinder B and are absorbed. (3) A variable time ( $t$ ) later, cylinder C is gated to ground potential, dumping the remaining electrons out that end along the magnetic-field lines to be collected.

A radially movable collector assembly behind a slot in the endplate collimates and collects the electrons at its radial ( $r$ ) and azimuthal ( $\theta$ ) position. At each dump the charge collected produces a voltage pulse, which is sampled and held for display on an  $x$ - $y$  recorder. This signal is proportional to the electron density  $n$ . The radial position of the collector is transduced and applied to the  $x$  axis of the recorder. By varying  $r$  we obtain  $n(r)$ , and changing the dump time yields  $n(r, t)$ . Examples of profiles taken in this manner are shown in Fig. 2(a). Notice the excellent "shot-to-shot" reproducibility evident from these data. A profile takes  $\sim 1$  min to generate while the repetition rate is 60/sec and thus thousands of shots have been used in its construction.

Several methods may be used to obtain the absolute magnitude of a radial profile. We have found that the most convenient and precise way is to measure the frequency of resonance transmission of the diocotron wave with lowest azimuthal-mode number. This frequency is proportional to the line density,<sup>10</sup>  $N(t) = \int_0^R dr' 2\pi r' n(r', t)$ . Some typical parameters of the  $t=0$  plasma are the following:  $\omega_{p0} = [n(0, 0)e^2/m\epsilon_0]^{1/2} \sim 10^8$  rad/sec;  $\omega_c = eB_0/m \sim 2 \times 10^9$  rad/sec; the average axial transit time is  $\sim 10^{-6}$  sec;  $\tau_f \sim 10^{-3}$  sec; and at base pressure the electron-neutral collision time

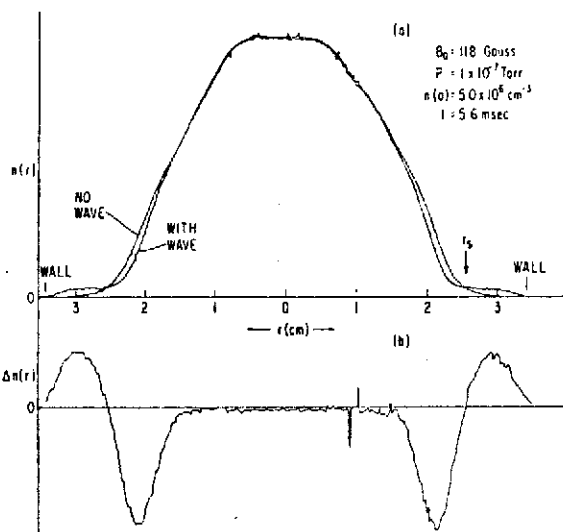


FIG. 2. (a) Radial density profiles taken with and without an externally launched diocotron mode. (b) Wave-induced density change taken electronically.

is  $\sim 10^{-3}$  sec.

It is useful to relate questions regarding transport of this single-charge-species plasma to canonical angular momentum,  $P_\theta$ . For a single electron  $p_{\theta i} = m(rv_\theta - r^2\omega_c/2)_i$ , where  $v_\theta$  is the azimuthal velocity component comprised of both the  $\vec{E} \times \vec{B}_0$  drift and the thermal motion. For  $r\omega_c \gg |v_{\theta 2}|$ , which is true for our plasmas,  $p_{\theta i} \approx -(m\omega_c/2)r_{gi}^2$  where  $r_{gi}$  is the radius of the guiding center. In the absence of external torques, conservation of total angular momentum requires that  $P_\theta \approx \sum_i p_{\theta i} \approx -(m\omega_c/2)\sum_i r_{gi}^2$  be constant. This says that if some electrons increase their average radial position others must decrease theirs. Since the initial average plasma radius is somewhat less than the wall radius this type of rearrangement can lead to loss of only a small fraction of the particles. To have gross transport out of the cylinder, an external torque must be applied. Intraplasma forces, such as electron-electron collisions or plasma instabilities, may only rearrange the electron distribution but not destroy the basic containment.<sup>11</sup> Torque can be applied by field imperfections but this effect is negligible on the time scale of the experiment discussed here.

An external torque can be applied to the plasma through electron collisions with background neutrals, which we have investigated by adding neutral gas to the system.<sup>4,5</sup> A detailed account of these transport results will appear in a future publication where they will also be compared to a recent kinetic-theoretical treatment.<sup>12</sup> For the

present experiment, the system is operated at its base pressure and the time scale for transport due to neutral collisions is slow compared to the effects of interest.

Another way to induce transport via an external torque is to launch a wave with an electric-field component perpendicular to  $\vec{B}$ . Diocotron waves<sup>6,7</sup> are low-frequency waves ( $\omega \ll \omega_p \ll \omega_c$ ) which propagate in a direction perpendicular to the magnetic field, having a first-order potential perturbation of the form  $\delta\varphi(r, \theta, t) = \psi(r) \exp(i l \theta - i \omega t)$ . It is possible for such a wave to be in resonance with the plasma drift motion at a particular radius  $r_s$ . This resonance occurs where  $\omega - l\omega_B(r_s) = 0$ , where  $\omega_B$  is the drift frequency due to the zero-order space-charge electric field:  $\omega_B(r) = -E(r)/rB_0$ ,  $E(r) = -(e/r\epsilon_0) \int_0^r dr' r' n(r')$ . In a zero-Larmor-radius linearized treatment, Briggs, Daugherty, and Levy have discussed<sup>7</sup> the analogy between such a resonance and the Landau resonance<sup>13</sup> of electron plasma waves with the velocity distribution function. In the next order, one expects such a resonance to cause spatial transport just as a single plasma wave can cause velocity-space transport.<sup>14</sup>

Radial density profiles taken with and without a launched diocotron ( $l=2$ ) are shown in Fig. 2(a). The wave was launched by applying an rf burst to two wall probes. These profiles are taken after the wave has essentially died away. The presence of the wave moves electrons outward, which of course means a change in  $P_\theta$  due to the torque applied through the wave. Shown in Fig. 2(b) is the wave-induced density change,  $\Delta n$ , taken electronically. The arrow marks  $r_s$  calculated from the density profile (no wave), showing that  $\Delta n$  goes through zero at  $r_s$ . This wave transport scales roughly as the peak power of the excited mode. Residual transport due to neutral collisions slowly washes out the  $\Delta n$  profile, which here decayed  $\sim 50\%$  after 8 msec.

This mode may be excited for only a narrow range in launched frequency ( $\omega/\Delta\omega \sim 40$ ), the central frequency determined by the density profile and magnetic-field strength. We have numerically calculated the real part of the mode frequency by using linear theory but neglecting resonant-particle effects. (Only for  $l=1$  is the frequency independent of the radial profile.) For  $l=2$  the calculation yields  $\omega = 3.37 \times 10^6$  rad/sec, a value within 2% of the mode frequency in the experiment. This calculation also yields the real part of the eigenfunction  $\psi(r)$ . We have also calculated the expected linear damping due to the resonant

particles using the standard quadratic-form expansion for weak damping.<sup>7</sup> This predicts the linear damping to be moderate ( $|\gamma|/\omega \sim 1/50$ ) in contrast to the observed damping which is an order of magnitude weaker.

Experimentally, the wave amplitude is set large enough to produce observable transport. This amplitude is sufficiently large that the linear damping mechanism is overcome and the resulting wave behaves nonlinearly. A clear demonstration of the nonlinear nature of the wave damping is shown in Fig. 3. Here we show the wave power received on a wall probe as a function of time after the transmitter turns on,  $t_w$ . The time that the transmitter is on is indicated. Curve *a* is the time history of the wave power which caused the transport shown in Fig. 2. Curve *b* is related to curve *a* by a standard attenuator-substitution experiment, wherein *b* was launched 12 dB down and the receiver gain upped by the same amount. Thus curve *a* represents a larger wave in the plasma and we see that larger waves decay more slowly. The decay time is proportional to the square root of the maximum amplitude of the received wave over a range of  $\sim 30$  dB in wave amplitude. A relatively large wave, with peak power near saturation with transmitter amplitude, was used in curve *a* in Fig. 3 in order to show transport clearly on the raw radial profiles of Fig. 2(a). Much smaller transport levels can be discerned with the  $\Delta n$  technique.

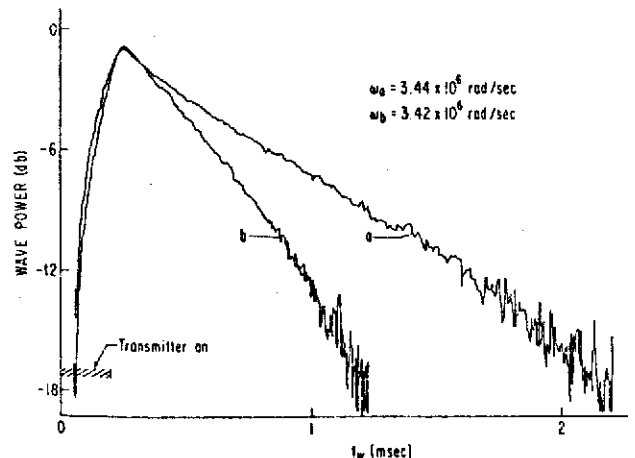


FIG. 3. Received wave power vs  $t_w$ , the time after transmitter turns on. Waves were launched with a 200- $\mu$ sec burst applied to two wall probes, each driven at 0.84 V rms for curve *a*. Curve *b* was launched 12 dB down with the receiver gain upped by the same factor. The receiver bandwidth is 650 KHz; the detector time constant is  $\sim 20$   $\mu$ sec.  $t_w = 0$  corresponds to  $t = 2.3$  msec.

These large-amplitude diocotron waves make the resonant electrons execute trapped orbits in space. The bounce frequency,  $\omega_B$ , of deeply trapped electrons is given by<sup>7</sup>  $\omega_B^2 = (l^2/r_e B_0) |\psi \partial \omega_B / \partial r|_{r=r_s}$ . For the wave levels used here the resonant electrons execute many trapped orbits during the duration of the wave. By knowing the shape of the eigenfunction  $\psi(r)$  we can obtain the absolute magnitude of the wave with a calibrated receiver since the power is proportional to  $|\partial \psi / \partial r|_{r=R}^2$ . As a reasonable approximation, using  $\psi$  found from the linear calculation we find  $\omega_B \sim 7 \times 10^5$  rad/sec for the wave level of curve *a* at its maximum. This gives  $\omega_B t_w \sim 10^3$  for the horizontal scan time in Fig. 3.

The apparent linearity of the maximums in the substitution experiment (Fig. 3) is misleading because the wave levels are nearing saturation with transmitter amplitude. Well below this level the wave responds as  $|\partial \psi / \partial r|_{r=R}^2 \sim t_w^2 A_T^3$  while the transmitter is on; here  $A_T$  is the transmitter amplitude. The frequencies of the waves in Fig. 3 differ slightly because the transmitter frequency exciting the largest wave depends mildly upon the transmitter amplitude. This effect is due to the modal frequency shift resulting from the modification of the profile.

In summary, we have found that the pure electron plasma is an excellent system in which to investigate transport across a strong magnetic field. In the absence of external torques, gross plasma containment is assured, thus allowing transport processes to be externally induced and isolated. The spatial transport due to a launched diocotron mode occurs at the radius for which the plasma  $\vec{E} \times \vec{B}_0$  drift motion is resonant with the wave. A linear calculation accurately predicts the real part of the modal frequency but also predicts the mode to be more heavily damped than is observed. The wave amplitudes are large enough to overcome the linear damping mechanism through trapping of the resonant electrons. The full nonlinear orbits must be used in a cal-

ulation of the actual damping and transport, for which we as yet have no theoretical description.

We wish to acknowledge many enlightening discussions with professor T. M. O'Neil. This research was supported by the National Science Foundation, Grant No. PHY73-05125-A03.

<sup>1</sup>A. W. Trivelpiece, *Comments Plasma Phys. Controlled Fusion* **1**, 57 (1972).

<sup>2</sup>R. C. Davidson, *Theory of Nonneutral Plasmas* (Benjamin, Reading, Mass., 1974).

<sup>3</sup>J. H. Malmberg and J. S. deGrassie, *Bull. Am. Phys. Soc.* **20**, 1239 (1975).

<sup>4</sup>J. S. deGrassie, J. H. Malmberg, and M. H. Douglas, *Bull. Am. Phys. Soc.* **20**, 1239 (1975).

<sup>5</sup>J. S. deGrassie, J. H. Malmberg, and M. H. Douglas, *Bull. Am. Phys. Soc.* **21**, 1115 (1976).

<sup>6</sup>R. H. Levy, *Phys. Fluids* **8**, 1288 (1965).

<sup>7</sup>R. J. Briggs, J. D. Daugherty, and R. H. Levy, *Phys. Fluids* **13**, 421 (1970).

<sup>8</sup>J. H. Malmberg and J. S. deGrassie, *Phys. Rev. Lett.* **25**, 577 (1975).

<sup>9</sup>This gating pulse is deliberately slowed down in order to avoid excitation of the diocotron wave of lowest azimuthal-mode number. The toroidal version of this mode has been observed in toroidal containment devices; see J. D. Daugherty, J. E. Eninger, and G. S. Janes, *Phys. Fluids* **12**, 2677 (1969); and also W. Clark, P. Korn, A. Mondelli, and N. Rostoker, *Phys. Rev. Lett.* **37**, 592 (1976).

<sup>10</sup>R. H. Levy, *Phys. Fluids* **11**, 920 (1968).

<sup>11</sup>This conservation law does not constrain gross transport in a charge neutral plasma since the contributions to  $P_\theta$  from the oppositely charged species can cancel in that case; i.e., electrons and ions cross the field lines together.

<sup>12</sup>T. M. O'Neil and M. H. Douglas, *Bull. Am. Phys. Soc.* **21**, 1115 (1976), and also to be published.

<sup>13</sup>L. Landau, *J. Phys. (U.S.S.R.)* **10**, 25 (1946).

<sup>14</sup>For a description of the velocity-space transport due to a single plasma wave, see J. H. Malmberg, T. H. Jensen, and T. M. O'Neil, in *Proceedings of the Third International Conference on Plasma Physics and Controlled Nuclear Fusion Research, Novosibirsk, U.S.S.R., 1968* (International Atomic Energy Agency, Vienna, Austria, 1969), Vol. I, p. 683.